LITERATURE CITED

Barber, J. R., "Intermolecular forces in the critical azeotropic system propane-perfluorocyclobutane: Description of forces in the vapor region via second virial coefficients and in the liquid region via internal pressure and internal force," Ph.D. Thesis, The Ohio State University (1968).

Barber, J. R., W. B. Kay and A. S. Teja, "A Study of the Volumetric and Phase Behavior of Binary Mixtures. Parts I and II of this paper.

Douslin, D. R., R. T. Moore and G. Waddington, "The Pressure-Volume-Temperature Properties of Perfluorocyclobutane: Equation of State, Virial Coefficients and Intermolecular Potential Energy Functions," *J. Phys. Chem.*, 63 (1959).

Leland, T. W. and P. S. Chappelear, "The Corresponding States Principle," *Ind. Eng. Chem.*, 60(7), 15 (1968).

McGlashan, M. L. and D. J. B. Potter, "An apparatus for the Measurement of the Second Virial Coefficients of Vapors: the Second Virial Coefficients of some n-alkanes and some mixtures of n-alkanes," *Proc. Roy. Soc.*, A267, 478 (1962).

Sengers, J. M. H. L., M. Klein and J. S. Gallaher, "Pressure-Volume-Temperature Relationships of Gases: Virial Coefficients," *The American Institute of Physics Handbook*, 3rd. ed., 4, 204 (1972).

Teja, A. S. and J. S. Rowlinson, "The Prediction of the Thermodynamic Properties of Fluids and Fluid Mixtures," *Chem. Eng. Sci.*, 28, 529 (1973).

Teja, A. S., "The Prediction of Azeotropic Behavior and Saturated Liquid Densities in the Carbon Dioxide-Ethane System," *AIChE J.*, 21 618 (1975).

Teja, A. S., "The Use of the Corresponding States Principle for Mixtures Containing Polar Components," *Ind. Eng. Chem. Fundam.*, 18, 435 (1979).

Manuscript received October 7, 1980, and accepted March 18, 1981.

Thinning of a Liquid Film as a Small Drop or Bubble Approaches a Solid Plane

When a small drop or bubble approaches a solid surface, a thin liquid film forms between them, drains, until an instability forms and coalescence occurs. A hydrodynamic theory is developed for the first portion of this coalescence process: the drainage of the thin liquid film while it is still sufficiently thick that the effects of London-van der Waals forces and electrostatic forces can be ignored. This theory describes the time rate of change of the film profile, given only the drop radius and the required physical properties. Predictions are compared with profiles measured by Platikanov (1964) for gas bubbles. It is concluded that, even with only a trace of surfactant present, the liquid-gas interface may be nearly immobile (tangential components of velocity are zero) and the surface viscosities will have little effect upon the drainage rate.

C.-Y. LIN

and

J. C. SLATTERY

Department of Chemical Engineering
Northwestern University
Evanston, IL 60201

SCOPE

The rate at which drops or bubbles suspended in a liquid coalesce is important to the preparation and stability of emulsions, of foams, and of dispersions; to liquid-liquid extraction; to the formation of an oil bank during the displacement of oil from a reservoir rock. On a smaller scale, when two drops (bubbles) in a liquid phase approach each other or when a drop (bubble) approaches a solid surface, a thin liquid film forms between them, drains, until an instability forms and coalescence occurs. We must understand the factors controlling the rate of coalescence.

In order to simplify the problem, we will consider only the first portion of this coalescence process as a drop approaches a solid wall: the drainage of the thin liquid film while it is still sufficiently thick that the effects of London-van der Waals forces and electrostatic forces can be ignored. Our objective is to develop a hydrodynamic theory for both pure and surfactant systems that decribes the configuration of the liquid film formed as a function of time and in this way predict the rate at which this film drains. We will not consider the development and growth of instabilities in these thin films that would lead to coalescence.

We will limit our attention to small drops or bubbles and to liquid films so thin that we may apply the Reynolds lubrication theory approximation.

Our analysis may be considered a refinement of that proposed by Hartland (1969).

CONCLUSIONS AND SIGNIFICANCE

Our theory for the drainage of a liquid film between a small drop and a solid surface, while employing the same basic differential equation (Eq. 52), is an improvement on Hartland's (1969) development. We require less a priori information, we have a more reliable initial condition, and our boundary conditions are in better agreement with experimental observations.

We have been able to accurately describe some of the experimental profiles measured by Platikanov (1964) for gas bubbles at short times.

Our theory is not only more complete but also more accurate than the estimates offered by Frankel and Mysels (1962). Their theory includes one free parameter; ours, none.

The comparison between our theory and the data of Platikanov (1964) for bubbles suggests that, even when there is only a trace of surfactant present, the liquid-gas interface may be nearly immobile. By immobile, we mean that the tangential

components of velocity are zero. This is consistent with our estimate of the interfacial tension gradient required to immobilize the water-air interface.

The same results apply to a liquid drop approaching a solid surface, so long as there is sufficient surfactant present that the liquid-liquid interface is immobile.

This work suggests that, in the presence of surfactants, the fluid-fluid interface will be immobile as a liquid film drains between a drop or bubble and a solid surface. Since velocity gradients can not exist within an immobile interface, our conclusion is that the interfacial viscosities will have little effect upon the rate at which a film drains prior to the development of an instability leading to coalescence. This does not preclude the possibility that the interfacial viscosities may stabilize a film in the latter stage of the drainage process and in this way retard coalescence. (There are no experimental data to suggest that the interfacial viscosities are different from zero in the absence of surfactants.)

INTRODUCTION

Coalescence of drops or bubbles in a liquid phase proceeds in two stages. For example, as a bubble approaches a solid surface, a liquid-gas interface, or another bubble, a thin liquid film is formed, which thins as the two interfaces are forced together. The rate at which this film thins is determined by the rate at which the liquid drains from it. When the film becomes sufficiently thin, the effects of London-van der Waals forces and of electrostatic forces become significant. These forces can act to either retard or enhance drainage. At some point in time, an instability develops, the film ruptures, and coalescence occurs. The critical film thickness at which rupture occurs is controlled by the stability of the film (Ivanov et al., 1970; Lang and Wilke, 1971). Our direct concern here will be with the rate at which a thin film drains while it is still sufficiently thick that the effects of London-van der Waals forces and electrostatic forces can be ignored. We will not be concerned with its stability.

Reynolds (1886) visualized this thin film as being formed between two parallel disks. But the assumption of a plane fluid-fluid interface contradicts the axial component of the jump momentum balance.

The thin film is not bounded by parallel planes. As a drop or bubble approaches an interface, it develops a dimple: the film is thicker at its center than at its rim (Derjaguin and Kussakov, 1939; Allan et al., 1961; Platikanov, 1964; Hartland, 1967, 1969; Hartland and Wood, 1973; Hodgson and Woods, 1969; Burrill and Woods, 1973). Models concerned with the shape of the film as a drop or bubble approaches a fluid-fluid interface have been discussed by Chappelear (1961), by Charles and Mason (1960), by Jeffreys and Hawksley (1965), and by Lang and Wilke (1971). Our concern here will be the simpler case of a drop or bubble approaching a solid surface.

Frankel and Mysels (1962) estimated the thinning rate at the center and at the rim of the film as a small drop approached a rigid plane. Their expression for the thinning rate at the rim is nearly equal to that predicted by the simple analysis of Reynolds (1886) and is in reasonable agreement with some of the measurements of Platikanov (1964; see also Figures 6, 8, and 9). Their predicted thinning rate at the center of the film is lower than that seen experimentally (Platikanov, 1964). (See Figures 6, 7, and 9.)

Hartland and Robinson (1977) developed a more detailed model for the draining rate at the center and at the rim of the film. The dimple was assumed to consist of two parabolas, with the radius of curvature at the apex varying with time in the central parabola and constant in the peripheral parabola. However, a priori knowledge was required of the radial position outside the dimple rim at which the film pressure equaled the hydrostatic pressure.

The first attempt at deriving the equations governing the film shape as a function of time was made by Hartland (1969, 1970). He analyzed the region between the center and the rim of the dimple, assuming that the shape of the drop beyond the rim did not change with time and that the configuration of the fluid-fluid interface at the center was a spherical cap. He proposed that the initial film profile be taken directly from experimental data. We will have more to say about this analysis later.

Dimitrov and Ivanov (1978) derived approximate solutions for the thinning rate at the center and at the rim of the film as a bubble approaches a solid surface. They argued that, for sufficiently thin liquid films, the liquid-gas interface was nearly a plane parallel to the solid. Experimental data suggest that this would be valid only as the thinning rate approaches zero (Platikanov, 1964). The expression they obtained can have the same form as that found by Reynolds (1886) with a different numerical coefficient.

The effects of surfactants upon coalescence have been studied by Radoev et al. (1974), by Ivanov and Dimitrov (1974), and by Barber and Hartland (1976). The influence of induced circulation in adjacent phases on the drainage of thin films has been discussed by Reed et al. (1974a,b) and by Riol et al. (1975). In all of these studies, the film thickness was assumed to be uniform.

In what follows, we develop a more complete hydrodynamic theory for the thinning of a liquid film between a bubble and a solid plane. The effects of surfactants are considered for the limiting case of an immobile liquid-gas interface. For this same limiting case, the results also apply to a liquid drop approaching a solid plane.

STATEMENT OF PROBLEM

Figure 1 shows a gas bubble approaching a solid plane. Our objective is to determine the rate at which the thin liquid film separating the bubble from the solid wall drains as a function of time.

In carrying out this computation, we will make a number of assumptions.

i) Viewed in the cylindrical coordinate system of Figure 1, the

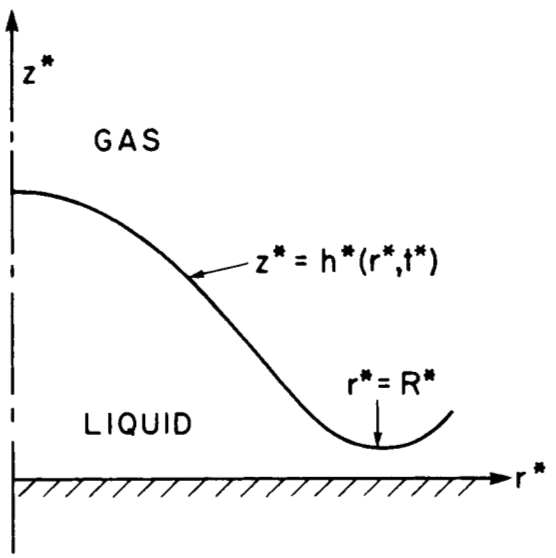

Figure 1. Configuration of a symmetric gas bubble approaching a solid plane.

gas-liquid interface is axisymmetric:

$$z^* = h^*(r^*, t^*) \tag{1}$$

ii) The dependence of h^* upon r^* is sufficiently weak that

$$\left(\frac{\partial h^*}{\partial r^*}\right)^2 \ll 1 \tag{2}$$

iii) Let R^* be the rim radius of the bubble:

$$\text{at } r^* = R^* = R^*(t^*): \frac{\partial h^*}{\partial r^*} = 0 \tag{3}$$

The Reynolds lubrication theory approximation applies in the sense that, if

$$h_0^* \equiv h^*(0, 0) \tag{4}$$

and

$$R_0^* \equiv R^*(0) \tag{5}$$

we will require

$$\left(\frac{h_0^*}{R_0^*}\right)^2 \ll 1 \tag{6}$$

iv) If there is no surfactant present, the interfacial tension is a constant independent of position on the interface and the surface viscosities are zero. We will refer to such an interface as being *mobile*.

v) If there is surfactant present, the tangential components of velocity $\underset{\sim}{v}^*$ at the gas-liquid interface are zero

$$\text{at } z^* = h^*: \underset{\sim}{P} \cdot \underset{\sim}{v}^* = 0 \tag{7}$$

and the interfacial tension gradient required to achieve this condition is very small. This latter statement is verified for the available experimental data. These interfaces will be termed *immobile*. In this limit, the results developed may also apply to a liquid drop approaching a solid plane, if it is reasonable to assume that all circulation within the liquid drop is suppressed.

vi) The effect of mass transfer on the velocity distribution is neglected.

vii) Viscous effects are neglected within the gas phase.

viii) The pressure p_0^* within the gas phase is independent of time and position.

ix) The liquid is an incompressible, Newtonian fluid, the viscosity of which is a constant.

x) All inertial effects are neglected.

xi) The effects of gravity, of London-van der Waals forces, and of electrostatic forces are neglected within the draining liquid film.

xii) The solid wall is stationary and

$$\text{at } z^* = 0: \underset{\sim}{v}^* = 0 \tag{8}$$

xiii) We will assume that pressure within the draining film approaches its local hydrostatic value beyond the rim where the Reynolds lubrication theory approximation (assumption iii) is still valid and that at this point the principal curvatures of the bubble are constants independent of time.

xiv) It has been observed (Platikanov, 1964) that, during the formation of the dimple as the bubble approaches the wall, the thinning rate at the rim is higher than that at the center of the dimple. After the dimple is completely established, the thinning rate at the rim is lower than that at the center. These experimental observations suggest that there is a time at which the thinning rate at the rim is equal to the thinning rate at the center. We will assume that at time $t^* = 0$ in our computations the thinning rate is independent of radial position. We will also assume that for $t^* > 0$ the thinning rate at the center is always greater than the thinning rate at the rim.

xv) The bubble or drop is sufficiently small that it may be assumed to be spherical

In constructing this development, we will find it convenient to work in terms of the dimensionless variables

$$r \equiv \frac{r^*}{R_0^*} \qquad z \equiv \frac{R_0^* z^*}{h_0^* R_0^*}$$

$$h \equiv \frac{R_0^* h^*}{h_0^* R_0^*} \qquad H \equiv H^* R_0^*$$

$$v_r \equiv \frac{v_r^*}{v_0^*} \qquad v_z \equiv \frac{R_0^* v_z^*}{h_0^* v_0^*}$$

$$p \equiv \frac{p^* - p_0^*}{\rho^*(v_0^*)^2} \qquad \gamma \equiv \frac{\gamma^*}{\gamma_0^*}$$

$$t \equiv \frac{t^* v_0^*}{R_0^*} \tag{9}$$

and dimensionless Reynolds, Weber, and capillary numbers

$$N_{\text{Re}} \equiv \frac{\rho^* v_0^* R_0^*}{\mu^*} \quad N_{\text{We}} \equiv \frac{\rho^*(v_0^*)^2 R_0^*}{\gamma_0^*} \quad N_{\text{ca}} \equiv \frac{\mu^* v_0^*}{\gamma_0^*} \tag{10}$$

Here H^* is the mean curvature of the gas-liquid interface, γ^* the surface tension, and γ_0^* the equilibrium surface tension. The characteristic speed v_0^* will be defined later.

Equation 1 suggests that we seek a solution in which the velocity distribution takes the form

$$\begin{aligned} v_r &= v_r(r,z,t) \\ v_z &= v_z(r,z,t) \\ v_\theta &= 0 \end{aligned} \tag{11}$$

Under these circumstances, the equation of continuity for an incompressible fluid

$$\text{div } \underset{\sim}{v}^* = 0 \tag{12}$$

says

$$\frac{1}{r}\frac{\partial}{\partial r}(r v_r) + \frac{\partial v_z}{\partial z} = 0 \tag{13}$$

The Navier-Stokes equation for an incompressible, Newtonian fluid with a constant viscosity reduces for creeping flow in the absence of gravity to

$$-\nabla p^* + \mu^* \text{ div } (\nabla \underset{\sim}{v}^*) = 0 \tag{14}$$

In the limit of assumption iii, the r-, θ-, and z-components of Eq. 14 are

$$\frac{\partial p}{\partial r} = \frac{1}{N_{\text{Re}}}\left(\frac{R_0^*}{h_0^*}\right)^2 \frac{\partial^2 v_r}{\partial z^2} \tag{15}$$

$$\frac{\partial p}{\partial \theta} = 0 \tag{16}$$

$$\frac{\partial p}{\partial z} = \frac{1}{N_{\text{Re}}}\frac{\partial^2 v_z}{\partial z^2} \tag{17}$$

This means that

$$\frac{\partial p}{\partial z} \ll \frac{\partial p}{\partial r} \tag{18}$$

and the dependence of pressure upon z will be neglected. Note that in arriving at Eqs. 15 and 17 it was not necessary to make any assumption about the magnitude of N_{Re} or the definition of v_0^*.

The jump mass balance (the requirement of mass conservation at the interface) and the jump mass balance for surfactant (the requirement of the mass balance for surfactant at the interface) are not required here, since we assume either that interfacial tension is a constant (assumption iv) or that the interfacial tension gradient is small (assumption v).

With either assumption iv or assumption v together with assumptions vi, vii, viii, x and xi, the jump momentum balance (the requirement of Euler's first law or Newton's second law at the interface; Deemer and Slattery, 1978) reduces to

$$\nabla_{(\sigma)}\gamma^* + 2H^*\gamma^*\underset{\sim}{\xi} - (\underset{\sim}{T}^* + p_0^*\underset{\sim}{I}) \cdot \underset{\sim}{\xi} = 0 \tag{19}$$

Here $\underset{\sim}{\xi}$ is the unit normal to the gas-liquid interface pointing into the gas phase; the surface gradient $\nabla_{(\sigma)}$ operation has been defined elsewhere (Wei et al., 1974; Briley et al., 1976). Under conditions of assumptions ii and iii, the r- and z- components of Eq. 19 assume the forms

$$\frac{\partial \gamma}{\partial r} - 2\frac{h_0^*}{R_0^*} H\gamma \frac{\partial h}{\partial r} - N_{We}\frac{h_0^*}{R_0^*} p \frac{\partial h}{\partial r} - N_{ca}\frac{R_0^*}{h_0^*}\frac{\partial v_r}{\partial z} = 0 \quad (20)$$

and

$$\frac{h_0^*}{R_0^*}\frac{\partial h}{\partial r}\frac{\partial \gamma}{\partial r} + 2H\gamma + N_{We}p - 2N_{ca}\frac{\partial v_z}{\partial z} + N_{ca}\frac{\partial v_r}{\partial z}\frac{\partial h}{\partial r} = 0 \quad (21)$$

The θ-component is satisfied identically. Adding $h_0^*/R_0^*\ \partial h/\partial r$ times Eqs. 21 to 20 and recognizing assumptions ii and iii, we have

$$\frac{\partial \gamma}{\partial r} - N_{ca}\frac{R_0^*}{h_0^*}\frac{\partial v_r}{\partial z} = 0 \quad (22)$$

and Eq. 20 implies

$$2H \cdot \gamma + N_{We}p = 0 \quad (23)$$

In arriving at Eqs. 22 and 23, it was not necessary to make any statement about the relative magnitudes of N_{ca} and N_{We} or the definition of v_0^*. But some statement is necessary in order to establish consistency with Eq. 21. Substituting Eq. 22 in 21, we have

$$2H\gamma + N_{We}p + 2N_{ca}\left(\frac{\partial v_r}{\partial z}\frac{\partial h}{\partial r} - \frac{\partial v_z}{\partial z}\right) = 0$$

It follows from Eqs. 48, 50, and 51, which depend upon Eq. 47, that

$$|2H\gamma| \gg |2N_{ca}\left(\frac{\partial v_r}{\partial z}\frac{\partial h}{\partial r} - \frac{\partial v_z}{\partial z}\right)|$$

in agreement with Eq. 23.

For a mobile interface, we will invoke assumption iv and use Eq. 22 in the form

$$\text{at } z = h: \frac{\partial v_r}{\partial z} = 0 \quad (24)$$

For an immobile interface, we will recognize assumptions iii and v to say instead

$$\text{at } z = h: v_r = 0 \quad (25)$$

and we will employ Eq. 22 to calculate the surface tension gradient required to create a rigid interface.

Since the effect of mass transfer on the velocity distribution is neglected (Assumption vi),

$$\text{at } z = h: v_z = \frac{\partial h}{\partial t} + \frac{\partial h}{\partial r} v_r \quad (26)$$

We will note that

$$\text{at } r = R: \frac{\partial h}{\partial r} = 0 \quad (27)$$

$$\text{at } r = 0: \frac{\partial h}{\partial r} = 0 \quad (28)$$

and

$$\text{at } r = 0: \frac{\partial p}{\partial r} = 0 \quad (29)$$

With Eqs. 18 and 23 together with assumptions ii and either iv or v, Eq. 29 implies

$$\text{at } r = 0: \frac{\partial H}{\partial r} = \frac{1}{2}\frac{h_0^*}{R_0^*}\left(-\frac{1}{r^2}\frac{\partial h}{\partial r} + \frac{1}{r}\frac{\partial^2 h}{\partial r^2} + \frac{\partial^3 h}{\partial r^3}\right) \quad (30)$$

$$= 0$$

An application of L'Hospital's rule shows us that

$$\text{at } r = 0: \frac{\partial^2 h}{\partial r^2} = \frac{1}{r}\frac{\partial h}{\partial r} \quad (31)$$

and Eq. 30 reduces to

$$\text{at } r = 0: \frac{\partial^3 h}{\partial r^3} = 0 \quad (32)$$

According to assumption xiii, there is a point $r = R_h > R$, where the pressure $p$within the draining film approaches the local hydrostatic pressure in the neighborhood of the bubble,

$$\text{as } r \to R_h: p \to p_h \quad (33)$$

Assumption xiii also requires that the two principal radii of curvature at this point be constants independent of time,

$$\text{at } r = R_h: \frac{\partial h}{\partial r} = \left(\frac{\partial h}{\partial r}\right)_{t=0} \quad (34)$$

$$\text{at } r = R_h: \frac{\partial^2 h}{\partial r^2} = \left(\frac{\partial^2 h}{\partial r^2}\right)_{t=0} \quad (35)$$

The initial time is to be chosen by requiring (assumption xiv)

$$\text{at } t = 0: \frac{\partial h}{\partial t} = \text{constant} \quad (36)$$

For the case of a bubble (phase B) of radius R_b^* freely rising through a continuous phase C to a solid surface under the influence of the buoyancy force, the integral momentum balance for the bubble requires

$$\int_{S^*} (\underset{\sim}{T}^{(C)*} + \mathcal{P}_h^{(C)*}\underset{\sim}{I}) \cdot \underset{\sim}{n}\, dA^* + \int_{R(B)^*} \rho^{(B)*}\underset{\sim}{b}^* dV^* = 0 \quad (37)$$

in which we have recognized that

$$\mathcal{P}_h^{(C)*} \equiv p_h^* + \rho^*\varphi^* = \text{a constant} \quad (38)$$

Here S^* is the cloased surface bounding the bubble and $R^{(B)*}$ is the region in space that it occupies. We are assuming that the interfacial tension gradient in the bubble surface is small (assumptions iv and v); this is confirmed below for the experimental data examined here. In this limit, the jump momentum balance Eqs. 22 and 23 suggests that the effect of the viscous forces in the continuous phase C can be neglected and we can rearrange the z component of Eq. 37 for a small spherical bubble (assumption xv) as

$$N_{We}\int_0^{R_h}(p - p_h)r\, dr = \frac{2}{3}\frac{\Delta\rho^* g^*(R_0^*)^2}{\gamma_0^*}(R_b)^3 \quad (39)$$

If R_f denotes the value of the dimple radius as time becomes large, we would expect that

$$\text{as } t \to \infty: p \to 0 \quad \text{for } 0 \le r \le R_f \quad (40)$$

and

$$\text{as } t \to \infty: p \to p_h \quad \text{for } r > R_f \quad (41)$$

Recognizing Eqs. 40 and 41, we find that Eq. 39 gives

$$\text{as } t \to \infty: R \to R_f = \left[-\frac{2}{N_{We}p_h}\right]^{1/2}\left[\frac{2}{3}\frac{\Delta\rho^* g^*(R_0^*)^2}{\gamma_0^*}\right]^{1/2}(R_b)^{3/2} \quad (42)$$

A sufficiently small bubble may be assumed to be spherical (assumption xv), which implies

$$p_h = -\frac{2}{N_{We}R_b} \quad (43)$$

and Eq. 42 simplifies to (Derjaguin and Kussakov, 1939)

$$\text{as } t \to \infty: R \to R_f = \left[\frac{2}{3}\frac{\Delta\rho^* g^*(R_0^*)^2}{\gamma_0^*}\right]^{1/2}(R_b)^2 \quad (44)$$

Given R_b^*, we determine R_f^* by requiring Eq. 44 to be satisfied; we identify $R_0^* = R_f^*/R_f$.

In the case of a bubble formed at the tip of a capillary tube and forced against a solid surface (Platikanov, 1964), an experimentalist might be expected to measure $p_h^* - p_0^*$. An analysis similar to that leading to Eq. 42 yields

$$\text{as } t \to \infty: R \to R_f = \left[(R_b)^2 + \frac{2R_b}{p_h N_{We}}\right]^{1/2} \quad (45)$$

with the assumption that the radius of the bubble is nearly equal to the radius of the capillary. Knowing $p_h^* - p_0^*$, we can determine R_f^* by demanding that Eq. 45 is satisfied; we identify $R_0^* = R_f^*/R_f$.

Finally, for the sake of simplicity let us define our characteristic speed

$$v_0^* \equiv \frac{\mu^*}{\rho^* R_0^*} \tag{46}$$

which means

$$N_{\mathrm{Re}} = 1, N_{\mathrm{We}} = N_{\mathrm{ca}} = \frac{\mu^{*2}}{\rho^* R_0^* \gamma_0^*} \tag{47}$$

Note that we have not used this definition for v_0^* or this definition for N_{Re} in scaling the Navier-Stokes equation to neglect inertial effects (assumption x). The scaling argument required to suggest a priori under what circumstances inertial effects can be ignored would be different, based perhaps on the initial value of the speed of displacement of the fluid-fluid interface calculated at the center of the film.

Our objective in what follows is to obtain a solution to Eqs. 13 and 15 consistent with Eqs. 8, 23, 26 through 28, 31 through 36, either Eq. 24 or 25, and the second portion of assumption xiv. For a bubble freely rising to the solid surface under the influence of the buoyancy force, R_b^* is measured, p_h is specified by Eq. 43, and R_f^* is chosen by demanding that as $t \to \infty$ or just prior to the development of an instability and coalescence Eq. 44 be satisfied. For a bubble formed on the tip of a capillary and forced against a solid surface, $p_h^* - p_0^*$ is measured, R_b^* is identified with the radius of the capillary, and R_f^* is chosen by requiring that, as $t \to \infty$ Eq. 45 be satisfied. In either case, we identify $R_0^* = R_f^*/R_f$.

Note that, in addition to physical properties, only one parameter is required: R_b^* in the case of a bubble freely rising to a solid surface or $p_h^* - p_0^*$ in the case of a bubble formed on the tip of a capillary tube.

SOLUTION

Integrating Eq. 15 twice consistent with Eq. 8 and either Eq. 24 or 25, we find in view of Eq. 47

$$v_r = \left(\frac{h_0^*}{R_0^*}\right)^2 \frac{\partial p}{\partial r}\left(\frac{z^2}{2} - \frac{1}{n} h z\right) \tag{48}$$

where

$$\begin{aligned} &\text{mobile interface:} \quad n = 1 \\ &\text{immobile interface:} \quad n = 2 \end{aligned} \tag{49}$$

Substituting Eq. 48 into 13, integrating once, and applying Eq. 8, we have

$$v_z = -\left(\frac{h_0^*}{R_0^*}\right)^2 \left[\left(\frac{z^3}{6} - \frac{z^2}{2n} h\right)\left(\frac{1}{r}\frac{\partial p}{\partial r} + \frac{\partial^2 p}{\partial r^2}\right) - \frac{z^2}{2n}\frac{\partial p}{\partial r}\frac{\partial h}{\partial r}\right] \tag{50}$$

Equations 23 with 47 and the appropriate expression for the dimensionless mean curvature H says

$$N_{\mathrm{ca}} p = -\frac{h_0^*}{R_0^*}\frac{1}{r}\frac{\partial}{\partial r}\left(r\frac{\partial h}{\partial r}\right) \tag{51}$$

In writing this, we have taken $\gamma = 1$ either by assumption iv or by assumption v.

Substituting Eqs. 48, 50 and 51 into 26 and rearranging, we see (Hartland, 1969)

$$-\frac{\partial h}{\partial t'} = \frac{1}{3} h^3 \left(\frac{1}{r^3}\frac{\partial h}{\partial r} - \frac{1}{r^2}\frac{\partial^2 h}{\partial r^2} + \frac{2}{r}\frac{\partial^3 h}{\partial r^3} + \frac{\partial^4 h}{\partial r^4}\right) + h^2 \frac{\partial h}{\partial r}\left(-\frac{1}{r^2}\frac{\partial h}{\partial r} + \frac{1}{r}\frac{\partial^2 h}{\partial r^2} + \frac{\partial^3 h}{\partial r^3}\right) \tag{52}$$

in which

$$t' \equiv \frac{t}{N_{\mathrm{ca}}}\left(\frac{h_0^*}{R_0^*}\right)^3 \left(\frac{3-n}{2n}\right) \tag{53}$$

Note that, after an application of L'Hospital's rule with full recognition of Eqs. 28, 31, and 32, we see

$$\text{limit } r \to 0: \quad -\frac{\partial h}{\partial t'} = \frac{8}{9} h^3 \frac{\partial^4 h}{\partial r^4} \tag{54}$$

Having been given N_{ca} in the form of the physical properties, we can carry out the integration of Eq. 52.

Our first objective is to calculate the initial configuration of the liquid-gas interface consistent with assumption xiv. Recognizing Eq. 36, we can use Eq. 54 to write Eq. 52 as

$$\left(\frac{\partial^4 h}{\partial r^4}\right)_{r=0} = \frac{3}{8} h^3 \left(\frac{1}{r^3}\frac{\partial h}{\partial r} - \frac{1}{r^2}\frac{\partial^2 h}{\partial r^2} + \frac{2}{r}\frac{\partial^3 h}{\partial r^3} + \frac{\partial^4 h}{\partial r^4}\right) + \frac{9}{8}\left(h^2 \frac{\partial h}{\partial r}\right)\left(-\frac{1}{r^2}\frac{\partial h}{\partial r} + \frac{1}{r}\frac{\partial^2 h}{\partial r^2} + \frac{\partial^3 h}{\partial r^3}\right) \tag{55}$$

We require that the result be consistent with Eqs. 28, 32, 33, and 27 in the form

$$\text{at } r = 1: \quad \frac{\partial h}{\partial r} = 0 \tag{56}$$

For a small bubble freely rising to a solid surface. Eq. 33 can be expressed as

$$\text{as } r \to R_h: \quad \frac{1}{r}\frac{\partial}{\partial r}\left(r\frac{\partial h}{\partial r}\right) \to \frac{2}{R_b^*}\frac{(R_0^*)^2}{h_0^*} \tag{57}$$

in which we have observed Eqs. 43 and 51. For a bubble formed on the tip of a capillary, Eq. 33 becomes in view of Eq. 51

$$\text{as } r \to R_h: \quad \frac{1}{r}\frac{\partial}{\partial r}\left(r\frac{\partial h}{\partial r}\right) \to -p_h N_{\mathrm{ca}} \frac{R_0^*}{h_0^*} = -\frac{p_h^* - p_0^* R_0^{*2}}{\gamma_0^* h_0^*} \tag{58}$$

In order to integrate a finite-difference form of Eq. 55, we replace Eq. 57 or 58 by

$$\text{at } r = 1: \quad \frac{\partial^2 h}{\partial r^2} = C \tag{59}$$

where C is a free parameter, the value of which will be determined shortly.

For each value of C, we can determine a tentative initial configuration of the film by integrating Eq. 55 consistent with Eqs. 28, 32, 56, and 59. The dimensionless radial position at which the pressure gradient becomes negligible is tentatively identified as R_h, subject to later verification that assumption ii is still satisfied at this point.

Equation 52 can be integrated consistent with each of these tentative initial configurations, Eqs. 28, 32, 34, and 35. Equation 27 permits us to identify R as a function of time; R_f is the value of R as $t' \to \infty$. We employed the Crank-Nicolson technique (Myers, 1971); accuracy was checked by decreasing the time and space intervals.

In addition to requiring that at time $t^* = 0$ the thinning rate is independent of radial position, assumption xiv demands that for $t^* > 0$ the thinning rate at the center is always greater than the thinning rate at the rim. Our numerical compuations indicate that there is a minimum value of the parameter C for which this condition is satisfied. This also corresponds to the maximum value of h_0^* for which the thinning rate at the center is always greater than the thinning rate at the rim for $t^* > 0$. We will choose this maximum value of h_0^* as our initial film thickness at the center.

For a bubble freely rising to the solid surface under the influence of the buoyancy force, R_b^* is measured and R_f^* is determined by Eq. 44. For a bubble formed on the tip of a capillary and forced against a solid surface, $p_h^* - p_0^*$ is measured and R_f^* is fixed by Eq. 45. In both cases, $R_0^* = R_f^*/R_f$.

We can determine h_0^* either from Eq. 57 for a bubble freely rising to the solid surface under the influence of the buoyancy force or from Eq. 58 for a bubble formed on the tip of a capillary and forced against a solid surface.

We must now check whether assumption ii is satsified at R_h; if it is satisifed here, it will be satisfied everywhere. It is desirable to choose R_h as large as possible, in order to make the pressure gradient at this point clearly negligible. But if R_h is assigned too large a value, assumption ii will be violated.

Finally, in the case of an immobile interface, we can examine assumption v that the interfacial tension gradient required to achieve this condition is very small. From Eqs. 22, 48, and 51, we have

$$\frac{\partial \gamma}{\partial r} = -\frac{1}{2}\left(\frac{h_0^*}{R_0^*}\right)^2 h \frac{\partial}{\partial r}\left[\frac{1}{r}\frac{\partial}{\partial r}\left(r\frac{\partial h}{\partial r}\right)\right] \tag{60}$$

This can be integrated with the observation that, since the surface tension gradient is proportional to the pressure gradient, from Eqs. 22 and 48,

$$\text{at } r = R_h\text{: } \gamma = 1 \tag{61}$$

RESULTS

For $R_h = 1.96$, we find

$$C = 5.05$$

$$R_f = 1.10$$

$$\text{at } r = R_h\text{: } \frac{\partial h}{\partial r} = 8.42$$

$$\text{at } r = R_h\text{: } \frac{1}{r}\frac{\partial}{\partial r}\left(r\frac{\partial h}{\partial r}\right) = 12.68$$

Figure 2 shows the dimensionless film thickness as a function of r and t'. The variation of pressure as a function of position and time in Figure 3 is similar to that calculated from experimental data by Hartland and Robinson (1977). Note that pressure and the configuration of the film are still functions of time beyond the rim: $R < r < R_h$. The dimensionless pressure distribution is consistent with Eqs. 40 and 41.

We have compared these computations with data for three systems studied by Platikanov (1964). He formed a small bubble on the tip of a capillary and forced it against a solid plane. Since he did not measure the bubble pressure $p_h^* - p_0^*$, we took R_f^* directly from his measured film profiles. We used (45) to determine $p_h N_{ca}$, recognizing Eq. 47. The bubble was assumed to be a

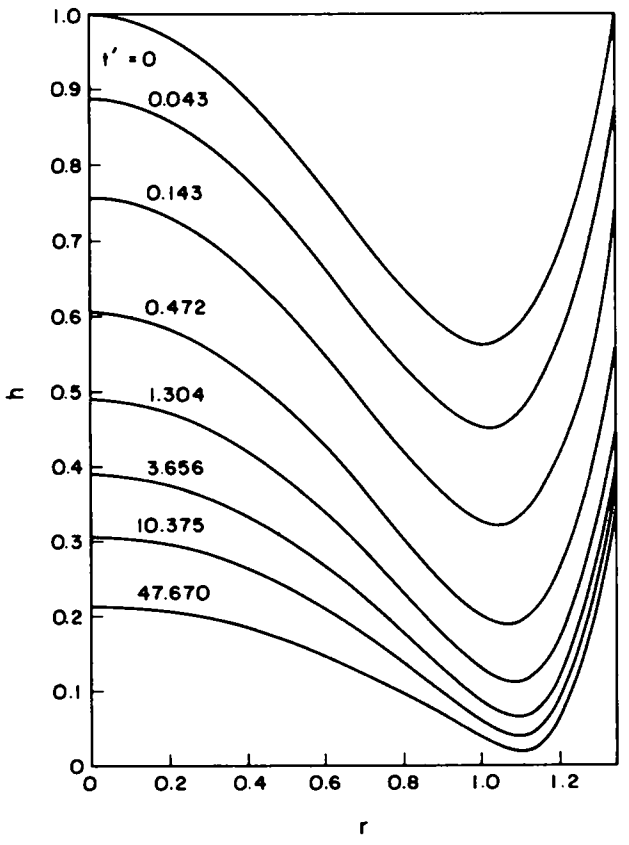

Figure 2. Dimensionless film thickness h as a function of dimensionless radial position and dimensionless time for $R_h = 1.96$.

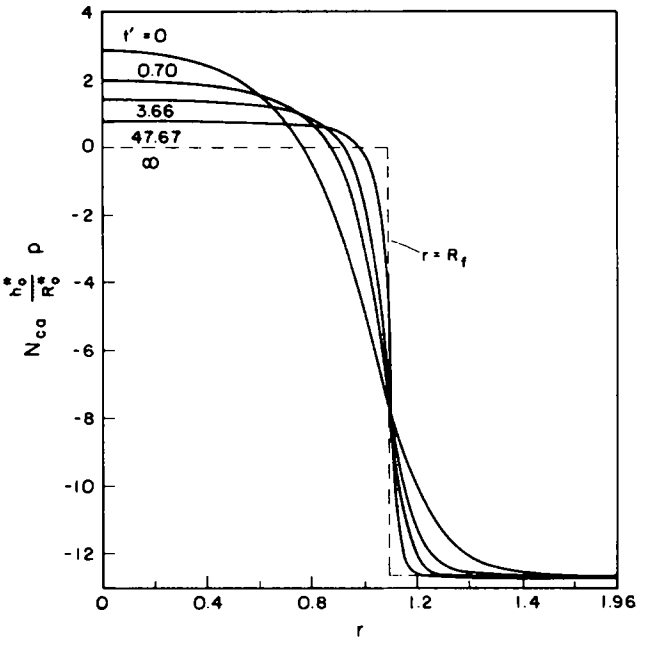

Figure 3. Dimensionless film pressure as a function of dimensionless radial position and dimensionless time for $R_h = 1.96$.

hemisphere whose radius R_b^* was the same as the radius of his capillary, 0.24 cm. Since his first measurements in all three cases were taken after our $t = 0$ (see Eq. 36), we related our time scale to his by matching his initial measurement of film thickness at the rim. As we shall demonstrate, we found it satisfactory to identify $R_h = 1.96$ for all of these systems.

For comparison, we also show the predictions of Frankel and Mysels (1962):

$$\text{at } r^* = 0\text{: } h^* = \left[\frac{0.0096 n^2 \mu^* R^{*6}}{\gamma^* R_b^*}\right]^{1/4} [t^* - t_0^*]^{-1/4} \tag{62}$$

$$\text{at } r^* = R^*\text{: } h^* = \left[\frac{0.090 n^2 \mu^* R^{*2} R_b^*}{\gamma^*}\right]^{1/2} [t^* - t_0^*]^{-1/2} \tag{63}$$

Note that with these relationships, the rim radius R^* is assumed to be a constant and t_0^* is an adjustable parameter.

0.1 N KCl Solution-Air

Platikanov (1964) reports observations for an air bubble forced against a solid surface through a continuous 0.1 N KCl solution:

$$\gamma_0^* = 7.27 \times 10^{-2} \text{ N/m and } \mu^* = 1.0 \times 10^{-3} \text{ Pa} \cdot \text{s}.$$

Since it is very difficult to produce and maintain uncontaminated aqueous solutions, we follow the suggestion of Platikanov (1964) in assuming that some surface-active material is present and $n = 2$. Figure 4 shows the results of our computations and the comparison with Platikanov's (1964) data. The experimental values of t^* are shown.

We find that at our $t = 0$ [Platikanov's (1964) $t^* = 0.30$ s] when the thinning rate is independent of position

$$h_0^* \equiv h^*(0,0) = 1.068 \times 10^{-4} \text{ cm}$$

and

$$\left(\frac{h_0^*}{R_0^*}\right)^2 = 7.04 \times 10^{-5}$$

which means that the Reynolds lubrication theory approximation (assumption iii) is applicable. The first reported experimental data are for a later time (his experimental $t^* = 1$ s) at which the centerline film thickness is 9.1×10^{-5} cm. Notice that the thinning rate is still nearly independent of radial position for his initial profile.

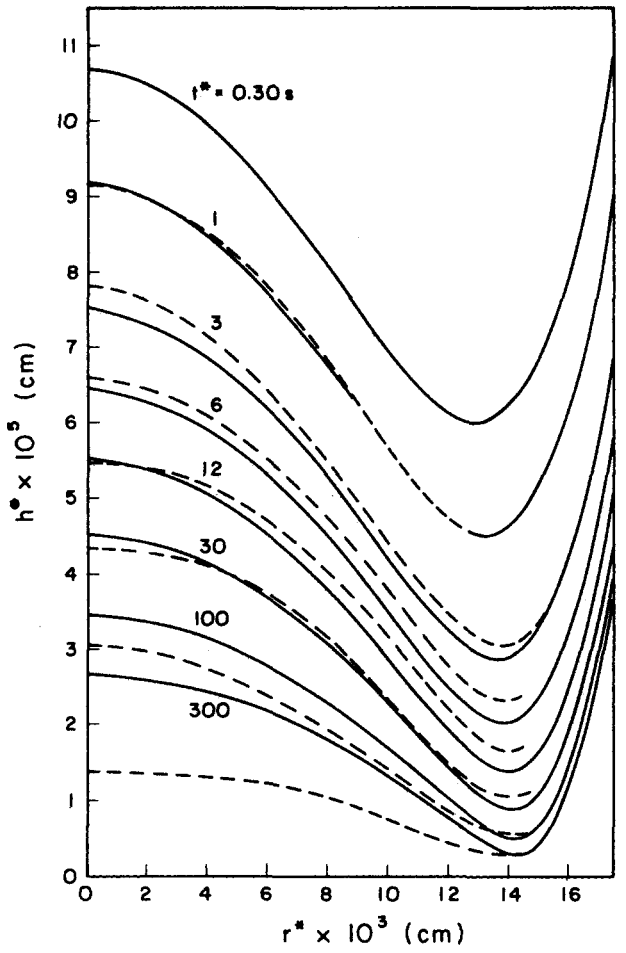

Figure 4. Comparison of the film profiles calculated using the present theory (solid lines) with those measured by Platikanov (1964, broken lines) for 0.1 N KCl solution-air interface. Here t^* represents Platikanov's experimental time scale, and $t^* = 0.30$ s corresponds to our $t = 0$.

$$\text{At } r = R_h = 1.96,$$

$$\left(\frac{\partial h^*}{\partial r^*}\right)^2 = 4.99 \times 10^{-3}$$

which means that assumption ii is still satisfied at this point.

Integrating Eq. 60 consistent with Eq. 61, we determine the surface tension distribution as a function of time shown in Figure 5. The surface tension gradients are small and decrease with time. The difference between the surface tension at the center and the equilibrium surface tension is only 3.00×10^{-5} N/m at 0.30 s and 1.21×10^{-6} N/m at 367 s. This suggests that the assumption of an immobile interface is reasonable even for a very dilute surfactant system.

The comparison between theory and experiment shown in Figure 4 is good for experimental times less than 100 s. At long times, we might expect the assumption of an immobile interface to fail.

Figure 6 compares the present results with the estimates of Frankel and Mysels (1962), Eqs. 62 and 63. The parameter t_0^* in these equations was determined by matching Platikanov's (1964) first measurement of film thickness at the rim. This gave a more favorable comparison between their estimates and the experimental data than was obtained by matching Platikanov's (1964) first measurement of centerline film thickness. Also shown in Figure 6 are the present results. Both theories give similar predictions of the thinning rate at the rim. The present results more accurately describe the thinning rate at the centerline.

Aniline-Air

Platikanov (1964) studied an air bubble forced against a solid

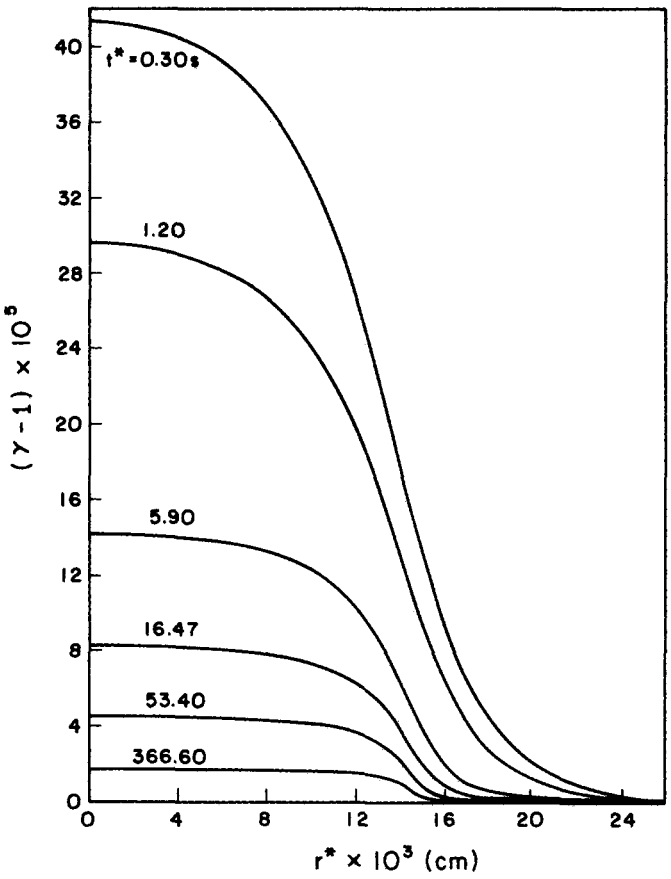

Figure 5. Dimensionless surface tension as a function of radial position and time for 0.1 N KCl solution-air interface. Here t^* represents Platikanov's experimental time scale.

surface where the continuous phase is aniline: $\gamma_0^* = 3.7 \times 10^{-2}$ N/m and $\mu^* = 4.48 \times 10^{-3}$ Pa·s.

Because of the likely presence of contaminants, we again assumed an immobile interface with $n = 2$.

From our computations, at our $t = 0$ [Platikanov's (1964) $t^* = 2.06$ s]

$$h_0^* = 1.39 \times 10^{-4} \text{ cm}$$

and

$$\left(\frac{h_0^*}{R_0^*}\right)^2 = 9.22 \times 10^{-5}$$

consistent with the Reynolds lubrication theory approximation (assumption iii). At $r = R_h = 1.96$,

$$\left(\frac{\partial h^*}{\partial r^*}\right)^2 = 6.53 \times 10^{-3}$$

which shows that assumption ii was not violated.

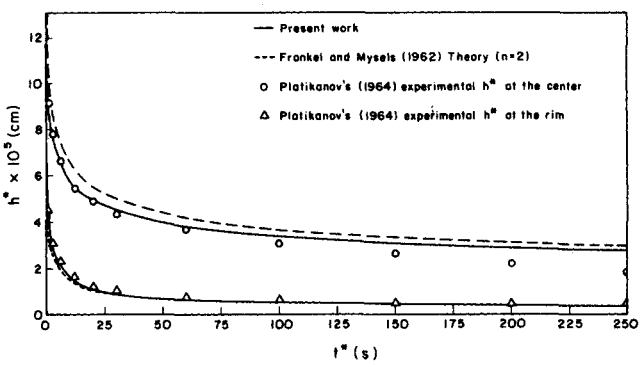

Figure 6. Comparisons of theories with experiment for 0.1 N KCl solution-air interface. Here t^* represents Platikanov's experimental time scale.

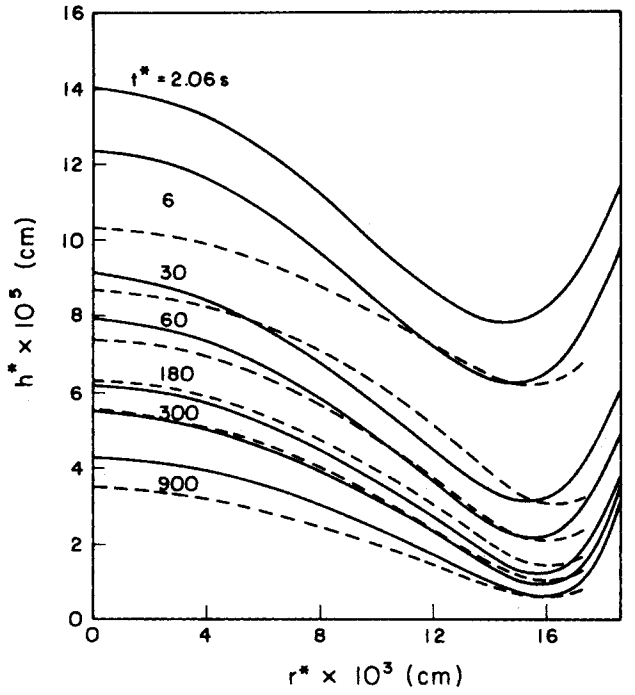

Figure 7. Comparison of the film profiles calculated using the present theory (solid lines) with those measured by Platikanov (1964, broken lines) for aniline-air interface. Here t^* represents Platikanov's experimental time scale, and $t^* = 2.06$ s corresponds to our $t = 0$.

Figure 7 compares the film profiles calculatd with the present theory with those measured by Platikanov (1964). The comparison is satisfactory for experimental times less than 400 s, again indicating a failure of the immobile interface assumption as the thinning rate slows.

Figure 8 presents a comparison of the present theory with the estimates Eqs. 62 and 63 by Frankel and Mysels (1962). The present theory again gives a better prediction of the thinning rate at the center of the film.

Ethanol-Air

Platikanov (1964) observed an air bubble forced against a solid surface through a continuous phase of ethanol: $\gamma_0^* = 2.23 \times 10^{-2}$ N/m and $\mu^* = 1.20 \times 10^{-3}$ Pa·s.

Since pure ethanol was used, we could expect a mobile interface for which $n = 1$.

We predict that at our $t = 0$ [Platikanov's (1964) $t^* = 0.68$ s]

$$h_0^* = 8.50 \times 10^{-5} \text{ cm}$$

and

$$\left(\frac{h_0^*}{R_0^*}\right)^2 = 5.60 \times 10^{-5}$$

consistent with the Reynolds lubrication theory approximation (assumption iii). At $r = R_h = 1.96$,

$$\left(\frac{\partial h^*}{\partial r^*}\right)^2 = 3.97 \times 10^{-3}$$

indicating that assumption ii was satisfied.

Figure 9 compares the film thicknesses at the center and at the rim as measured by Platikanov (1964) with the predictions of the present theory as well as the estimates of Frankel and Mysels (1962), Eqs. 62 and 63. While the present theory is superior to Eqs. 62 and 63, it fails to explain the observed rapid rate of thinning.

Platikanov (1964) suggested that the rapid thinning rate might be due to a positive disjoining pressure (an external force acting on the interface, possibly attributable to Van der Waals forces or the effect of an electrical double layer; Sheludko, 1967; Lee and Hodgson, 1968; Murdoch and Leng, 1971). A film might drain more rapidly, if it were tilted (Jeffreys and Hawksley, 1965; Hartland, 1969); but the experimental data show a symmetric dimple. The drainage rate might also be enhanced by a positive surface tension gradient, but this supposes a temperature or concentration profile in the liquid-gas interface not readily anticipated from the description of the experiment.

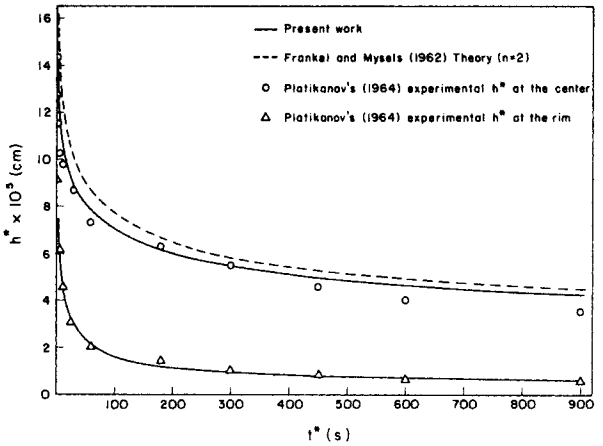

Figure 8. Comparisons of theories with experiment for aniline-air interface. Here t^* represents Platikanov's experimental time scale.

DISCUSSION

Although the governing differential Eq. 52 is the same, there are several major differences between the present theory and that described by Hartland (1969).

Hartland assumed a spherical cap at the center of the liquid film, because Eq. 52 is indeterminate at this point. We were able to apply L'Hospital's rule to obtain the thinning rate at the center (Eq. 54).

Hartland obtained the initial film profile directly from the experimental data. We calculated it from Eq. 55, reducing our requirement for *a priori* information. We did attempt to follow Hartland's prescription to start with the initial experimental film profile, but we were unable to complete the computations. Any given set of experimental data will not be completely consistent with Eq. 52: numerically, the initial thinning rates will be positive at some radial positions and negative at others, making the integration of Eq. 52 impossible.

Hartland assumed that the rim or dimple radius is independent of time and he integrated Eq. 52 from the centerline to a point immediately beyond the rim radius where the drop shape was assumed to be independent of time. We allow the rim radius to change with time and we integrate Eq. 52 from the center to a

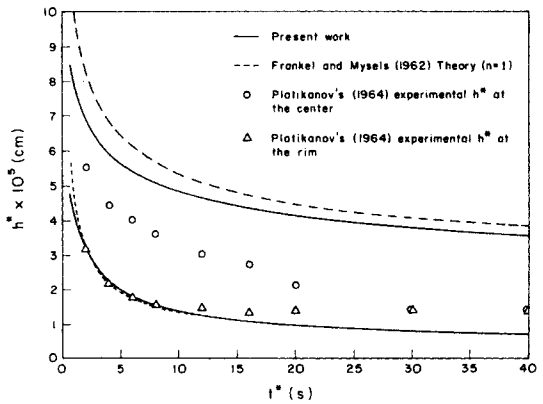

Figure 9. Comparisons of theories with experiment for ethanol-air interface. Here t^* represents Platikanov's experimental time scale.

point where the pressure can be assumed equal to the hydrostatic pressure. Hartland's approach results in a nearly constant pressure at the rim. Experimental results (Hartland and Robinson, 1977) indicate a positive pressure gradient at the rim in agreement with our computations, such as those shown in Figure 3.

Hartland also reported measured film profiles for large drops to which the theory developed here does not apply. Not only is assumption xv not satisfied, but also assumption ii is violated just beyond the rim where the pressure is less than the hydrostatic pressure.

The comparisons shown in Figures 6, 8, and 9 suggest that the present work is a relatively minor improvement over the simple result of Frankel and Mysels (1962) shown in (62) and (63). In fact, there are two important improvements. First, the Frankel and Mysels (1962) result contains an adjustable parameter t_0^* that has no physical significance. In the present theory, time is measured relative to the time at which the thinning rate is independent of radial position very early in the formation of the thin film. Second, the present theory is more complete in the sense that the entire configuration of the draining film can be described as a function of time, not just the thickness of the film at the center and at the rim.

ACKNOWLEDGMENT

The authors are grateful for financial support by the U.S. Department of Energy (Contract No. DE-AC19-79BC10068).

NOTATION

$\underset{\sim}{b}^*$ = acceleration of gravity
C = a parameter in Eq. 59
g^* = magnitude of acceleration
h^* = film thickness
h = dimensionless film thickness defined by Eq. 9
h_0^* = film thickness at $t^* = 0$ and $r^* = 0$
H^* = mean curvature of the gas-liquid interface
H = dimensionless mean curvature of the gas-liquid interface defined by Eq.9
$\underset{\approx}{I}$ = identity tensor that transforms every spatial vector field into itself
n = a parameter defined by Eq. 49
$\underset{\sim}{n}$ = unit normal to bubble surface pointing into continuous liquid phase
N_{ca} = capillary number defined byEq. 10
N_{Re} = Reynolds number defined by Eq. 10
N_{We} = Weber number defined by Eq. 10
p^* = pressure in liquid film
p = dimensionless pressure, defined by Eq. 9
$\underset{\approx}{P}$ = projection tensor that transforms any vector on the interface into its tangential component
p_h^* = hydrostatic pressure in the continuous liquid phase
p_h = dimensionless hydrostatic pressure
p_0^* = pressure within the gas phase
r^* = cylindrical coordinate
$\wp_h^{(c)*}$ = defined by Eq. 38
r^* = cylindrical coordinate
r = dimensionless cylindrical coordinate defined by Eq. 9
R^* = rim radius of the bubble
R = dimensionless rim radius defined as R^*/R_0^*
R_b^* = radius of the bubble
R_b = dimensionless radius of the bubble defined as R_b^*/R_0^*
R_f^* = dimple radius as $t \to \infty$ or just prior to the development of an instability and coalescence
R_f = dimensionless dimple radius as $t \to \infty$ or just prior to the development of an instability and coalescence, defined as R_f^*/R_0^*
R_h = dimensionless radial position where the pressure p within the draining film approaches the local hydrostatic pressure in the neighborhood of the bubble
R_0^* = rim radius of the bubble at $t^* = 0$
$R^{(B)*}$ = region occupied by bubble
S^* = surface of bubble
t^* = time
t = dimensionless time defined by Eq. 9
t' = dimensionless time defined by Eq. 53
t_0^* = an adjustable parameter in Eqs. 62 and 63
$\underset{\sim}{\underset{\sim}{T}}^*$ = stress tensor
$\underset{\sim}{\underset{\sim}{T}}^{(c)*}$ = stress tensor for continuous liquid phase
$\underset{\sim}{u}^*$ = velocity of a point on the surface with a fixed set of surface coordinates (Deemer and Slattery, 1978)
$\underset{\sim}{v}^*$ = velocity vector
v_r^* = r^* component of velocity vector $\underset{\sim}{v}^*$
v_r = dimensionless r^* component of velocity vector $\underset{\sim}{v}^*$ defined by Eq. 9
v_z^* = z^* component of velocity vector $\underset{\sim}{v}^*$
v_z = dimensionless z^* component of velocity vector $\underset{\sim}{v}^*$ defined by Eq. (9)
v_θ = dimensionless θ component of velocity vector $\underset{\sim}{v}^*$
v_0^* = characteristic speed defined by Eq. 46
z^* = cylindrical coordinate
z = dimensionless cylindrical coordinate defined by Eq. 9

GREEK LETTERS

γ^* = surface tension
γ = dimensionless surface tension defined by Eq. 9
γ_0^* = equilibrium surface tension
θ = cylindrical coordinate
μ^* = bulk viscosity of liquid film
ρ^* = density of liquid film
$\rho^{(B)*}$ = density of bubble
$\Delta\rho^*$ = $\rho^* - \rho^{(B)*}$
$\underset{\sim}{\xi}$ = unit normal to the gas-liquid interface pointing into the gas phase
φ^* = potential energy per unit mass; $\underset{\sim}{b}^* = -\nabla\varphi^*$

OTHERS

div = divergence operation
∇ = gradient operator
$\nabla_{(\sigma)}$ = surface gradient operator (Wei et al., 1974; Briley et. al., 1976)
dA^* = indicating that an area integration is to be performed
dV^* = indicating that a volume integration is to be performed

LITERATURE CITED

Allan, R. S., G. E. Charles, and S. G. Mason, "The Approach of Gas Bubbles to a Gas/Liquid Interface," *J. Colloid Sci.*, **16**, 150 (1961).

Barber, A. D., and S. Hartland, "The Effects of Surface Viscosity on the Axisymmetric Drainage of Planar Liquid Films," *Can. J. Chem. Eng.*, **54**, 279 (1976).

Briley, P. B., A. R. Deemer, and J. C. Slattery, "Blunt Knife-Edge and Disk Surface Viscometers," *J. Colloid Interface Sci.*, **56**, 1 (1976).

Burrill, K. A., and D. R. Woods, "Film Shapes for Deformable Drops at Liquid-Liquid Interfaces II. The Mechanisms of Film Drainage," *J. Colloid Interface Sci.*, **42**, 15 (1973).

Chappelear, D.C., "Models of a Liquid Drop Approaching an Interface," *J. Colloid Sci.*, **16**, 186 (1961).

Charles, G. E., and S. G. Mason, "The Coalescence of Liquid Drops with Flat Liquid-Liquid Interfaces," *J. Colloid Sci.*, **15**, 236 (1960).

Deemer, A. R., and J. C. Slattery, "Balance Equations and Structural Models for Phase Interfaces," *Int. J. Multiphase Flow*, **4**, 171 (1978).

Derjaguin, B., and M. Kussakov, "Anomalous Properties of Thin Polymolecular Films," *Acta Physicochim. URSS*, **10**, 25 (1939).

Dimitrov, D. S., and I. B. Ivanov, "Hydrodynamics of Thin Liquid Films. On the Rate of Thinning of Microscopic Films with Deformable Interfaces," *J. Colloid Interface Sci.*, **64**, 97 (1978).

Ekserova, D., I. Ivanov, and A. Sheludko, "The Independence of Depth and Diameter in Equilibrated Free Films," *Res. Surf. Forces, Proc. Conf., 2nd, 1964*, p. 144, Plenum, New York (1966).

Frankel, S. P., and K. J. Mysels, "On the 'Dimpling' during the Approach of Two Interfaces," *J. Phys. Chem.*, **66**, 190 (1962).

Hartland, S., "The Coalescence of a Liquid Drop at a Liquid-Liquid In-

terface Part II: Film Thickness," *Trans. Inst. Chem. Eng.*, **45**, T102 (1967).
Hartland, S., "The Profile of the Draining Film beneath a Liquid Drop Approaching a Plane Interface," *Chem. Eng. Prog. Symp. Ser.*, No. 91, **65**, 82 (1969).
Hartland, S., "The Profile of the Draining Film between a Fluid Drop and a Deformable Fluid-Liquid Interface," *Chem. Eng. J.*, (London), **1**, 67 (1970).
Hartland, S., and J. D. Robinson, "A Model for an Axisymmetric Dimpled Draining Film," *J. Colloid Interface Sci.*, **60**, 72 (1977).
Hartland, S., and S. M. Wood, "The Effect of Applied Force on Drainage of the Film between a Liquid Drop and Horizontal Surface," *AIChE J.*, **19**, 810 (1973).
Hodgson, T. D., and D. R. Woods, "The Effect of Surfactants on the Coalescence of a Drop at an Interface II," *J. Colloid Interface Sci.*, **30**, 429 (1969).
Ivanov, I. B., and D. S. Dimitrov, "Hydrodynamics of Thin Liquid Films: Effect of Surface Viscosity on Thinning and Rupture of Foam Films," *Colloid Polym. Sci.*, **252**, 982 (1974).
Ivanov, I. B., B. Radoev, E. Manev, and A. Scheludko, "Theory of the Critical Thickness of Rupture of Liquid Films," *Trans.* Faraday Soc., **66**, 1262 (1970).
Jeffreys, G. V., and J. L. Hawksley, "Coalescence of Liquid Droplets in Two-Component-Two-Phase Systems: Part 1. Effect of Physical Properties on the Rate of Coalescence," *AIChE J.*, **11**, 413 (1965).
Lang, S. B., and C. R. Wilke, "A Hydrodynamic Mechanism for the Coalescence of Liquid Drops. I. Theory of Coalescence at a Planar Interface," *Ind. Eng. Chem. Fundam.*, **10**, 329 (1971).
Lee, J. C., and T. D. Hodgson, "Film Flow and Coalescence-I. Basic Relations, Film Shape and Criteria for Interface Mobility," *Chem. Eng. Sci.*, **23**, 1375 (1968).
Murdoch, P. G., and D. E. Leng, "The Mathematical Formulation of Hydrodynamic Film Thinning and its Application to Colliding Drops Suspended in a Second Liquid-II," *Chem. Eng. Sci.*, **26**, 1881 (1971).
Myers, G. E., *Analytical Methods in Conduction Heat Transfer*, p. 274, McGraw-Hill, New York (1971).
Platikanov, D., "Experimental Investigation on the 'Dimpling' of Thin Liquid Films," *J. Phys. Chem.*, **68**, 3619 (1964).
Radoev, B. P., D. S. Dimitrov, and I. B. Ivanov, "Hydrodynamics of Thin Liquid Films: Effect of the Surfactant on the Rate of Thinning," *Colloid Polym. Sci.*, **252**, 50 (1974).
Reed, X. B., Jr., E. Riolo, and S. Hartland, "The Effect of Hydrodynamic Coupling on the Axisymmetric Drainage of Thin Films," *Int. J. Multiphase Flow*, **1**, 411 (1974a).
Reed, X. B., Jr., E. Riolo, and S. Hartland, "The Effect of Hydrodynamic Coupling on the Thinning of a Film between a Drop and its Homophase," *Int. J. Multiphase Flow*, **1**, 437 (1974b).
Reynolds, O., "On the Theory of Lubrication," *Philos. Trans. R. Soc. London Ser. A*, **177**, 157 (1886).
Riolo, E., X. B. Reed, Jr., and S. Hartland, "The Effect of Hydrodynamic Coupling on the Steady Drainage of a Thin Film between a Solid Sphere Approaching a Fluid-Fluid Interface," *J. Colloid Interface Sci.*, **50**, 49 (1975).
Sheludko, A., "Thin Liquid Films," *Adv. Colloid Interface Sci.*, **1**, 391 (1967).
Wei, L. Y., W. Schmidt, and J. C. Slattery, "Measurement of the Surface Dilatational Viscosity," *J. Colloid Interface Sci.*, **48**, 1 (1974).

Manuscript received October 16, 1979; revision received December 15, 1980, and accepted April 23, 1981.

Experimental Determination of the Light Distribution in a Photochemical Reactor:

Influence of the Concentration of an Absorbing Substance on This Profile

Knowledge of the local distribution of the light energy, in a photochemical reactor in the presence of an absorbing substance which reacts at a rate of order different from one with respect to the adsorbed light intensity, is important in order to calculate the mean rate of reaction and the design of the reactor. Here we report a simple method for the determination of this profile as a function of the concentration of an absorbing substance and we compare the results obtained with the models of emission from the literature. A semi-empirical model accounting for our experimental results is presented.

A. TOURNIER and X. DEGLISE

Laboratoire de Photochimie Appliquée
Université de Nancy I
54037 NANCY Cedex, France

and

J. C. ANDRE and M. NICLAUSE

Laboratoire de Chimie Générale
E.N.S.I.C.
54042 NANCY Cedex, France

SCOPE

Photochemical reactions have been studied extensively in both university and industrial laboratories, in particular reactions of order 1 with respect to the absorbed light intensity (photonitrosation of cyclohexane, for example, Fischer, 1974) or of order ½ such as the chain reactions of photochlorination or of photo-oxidation (Deglise, 1968; André, 1971; Tournier, 1978).

In cases where the reaction is 1st order, knowledge of the mean number of photons absorbed in the reactor per second is sufficient to account for the rate of reaction, and moreover in general the photoreactor is designed on the basis of heat transfer phenomena (depending on the endo- or exo-thermicity of the reaction).

On the other hand, when the order is different from 1, and when the chemical reaction involves other reactions between unstable species (excited electronic states, free radicals, ion-radicals, etc. . . .) only knowledge of the absorption profile allows us to account for the rate of formation of these species. Thus, the concentration of different unstable species is no longer homogeneous in the volume of the reactor, and a concentration